

AN EXPLICIT NEURAL NETWORK CONSTRUCTION FOR PIECEWISE CONSTANT FUNCTION APPROXIMATION

KAILIANG WU AND DONGBIN XIU*

Abstract. We present an explicit construction for feedforward neural network (FNN), which provides a piecewise constant approximation for multivariate functions. The proposed FNN has two hidden layers, where the weights and thresholds are explicitly defined and do not require numerical optimization for training. Unlike most of the existing work on explicit FNN construction, the proposed FNN does not rely on tensor structure in multiple dimensions. Instead, it automatically creates Voronoi tessellation of the domain, based on the given data of the target function, and piecewise constant approximation of the function. This makes the construction more practical for applications. We present both theoretical analysis and numerical examples to demonstrate its properties.

Key words. feedforward neural network, hidden layer, constructive approximation, Voronoi diagram.

1. Introduction. Feedforward neural network (FNN) has attracted wide attention in recent years, largely due to the many successes it brings to machine learning and artificial intelligence. There are an exceedingly large number of literature devoted to various aspects of FNN, particularly on their performance and algorithm design.

Most of the existing mathematical studies on FNN focus on single-hidden-layer FNN and its ability to approximate unknown target functions. The earlier theoretical results established that single-hidden-layer FNN is capable for approximating functions with arbitrary accuracy, see, for example, [7, 11, 2]. Efforts have then been made to explicitly constructive single-hidden-layer FNNs, where the weights and thresholds are explicitly specified and not solved numerically by a certain optimization procedure. These explicitly defined single-hidden-layer FNNs provide very useful, from the mathematical perspective, constructive proofs for the existence of FNNs for function approximation. One of the earliest constructions is the work in [4]. Since then, several other constructions have been presented, many of which are based on variations of the Cardaliaguet-Euvrard operator from [4]. These work include [1, 3, 5, 6, 9], to name a few. A common feature of these work is that the construction is typically based on a univariate formulation, for example, the Cardaliaguet-Euvrard operator [4] in 1D. To generalize to multivariate functions, tensor product is employed. The complexity of the constructions thus grows exponentially in high dimensions. Consequently, although these results are useful from the mathematical view point, they do not provide practical tools for applications.

In this paper, we present a new explicit construction of FNN for multivariate function approximation. A distinct feature of the proposed construction is that it does not utilize tensor structure in multiple dimensions. Instead, the network creates a piecewise constant approximation for any given function based the available data. The construction uses exclusively the threshold function, also known as hard limiter or binary function, as the activation function. The weights and thresholds in the network are explicitly defined, and we prove that the “pieces” in the piecewise constant approximation form a Voronoi diagram (cf. [10]) of the domain. Suppose one is given n sample data of the unknown target function, the proposed FNN then provides a piecewise constant approximation based n Voronoi cells of the underlying domain. We

*Department of Mathematics, The Ohio State University, Columbus, OH 43210, USA.
wu.3423@osu.edu, xiu.16@osu.edu.

also provides an error estimate of the approximation. Due to the explicit construction, the weights and thresholds of the FNN can be easily evaluated, thus avoiding a potentially expensive numerical optimization procedure for their training. This, along with the non-tensor structure of the construction, makes the proposed FNN a practical tool for applications, as it works with arbitrarily given data in arbitrary dimensions. We demonstrate the effectiveness of the FNN using several numerical examples, which also verify the error convergence from the theoretical estimate. In the current construction, which is perhaps one of the most intuitive ones, the network uses two hidden layers with (at most) n^2 neurons. Similar FNNs with less number of neurons are possible, by using more involved network structures. This shall be investigated in future studies. The proposed FNN is not only another (and new) constructive proof for the universal approximation property of FNNs, but also a practical tool for real data.

This paper is organized as follows. Upon a brief setup of the problem in Section 2, we present the explicit FNN construction in Section 3, which also includes its theoretical analysis. Numerical examples are then presented in Section 4 to demonstrate the properties of the FNN.

2. Setup. Consider the problem of approximating an unknown function $f : D \rightarrow \mathbb{R}$ using its samples, where $D \subseteq \mathbb{R}^d$, $d \geq 1$. Let $\mathbf{x} = (x_1, \dots, x_d)$ be the coordinate and

$$\left(\mathbf{x}^{(1)}, f^{(1)}\right), \dots, \left(\mathbf{x}^{(n)}, f^{(n)}\right), \quad n > 1, \quad (2.1)$$

be a set of training data, where $\mathbf{x}^{(k)} \in D$ are the location of the data samples and

$$f^{(k)} = f(\mathbf{x}^{(k)}) + \epsilon_k, \quad k = 1, \dots, n,$$

are the sample data, with $\epsilon_k \geq 0$ being (possible) observation error. We consider only the nontrivial case of $n > 1$.

3. Construction of the FNN. In this section, we present our construction of the feedforward neural network (FNN) with two hidden layers. We first present the detail of its structure and then prove that it provides a piecewise constant approximation for any target function $f : \mathbb{R}^d \rightarrow \mathbb{R}$.

3.1. The construction. The structure of the FNN is illustrated in Figure 3.1. It consists of an input layer, which has $d \geq 1$ neurons corresponding to the d -variate input signal, and an output layer with one neuron, as the function under consideration is $f : \mathbb{R}^d \rightarrow \mathbb{R}$. This is the standard setup for most of the FNN.

We will use exclusively the threshold function, also known as the step function, hard limiter function, binary function, etc, as the activation function

$$s(x) = \begin{cases} 1, & x \geq 0, \\ 0, & x < 0. \end{cases} \quad (3.1)$$

3.1.1. First hidden layer. The first hidden layer consists of $n(n-1)$ neurons, where $n > 1$ is the number of training samples. We shall divide the neurons into n groups, with each group corresponding to a training sample. Each group then includes $(n-1)$ neurons, thus making the total number of neurons in the first hidden layer $n(n-1)$. We shall use $N^{(1)}$ to denote the neurons in the first hidden layer and label them with two indices in the following way,

$$N_{k,j}^{(1)}, \quad 1 \leq k \leq n, \quad 1 \leq j \leq n, \quad j \neq k,$$

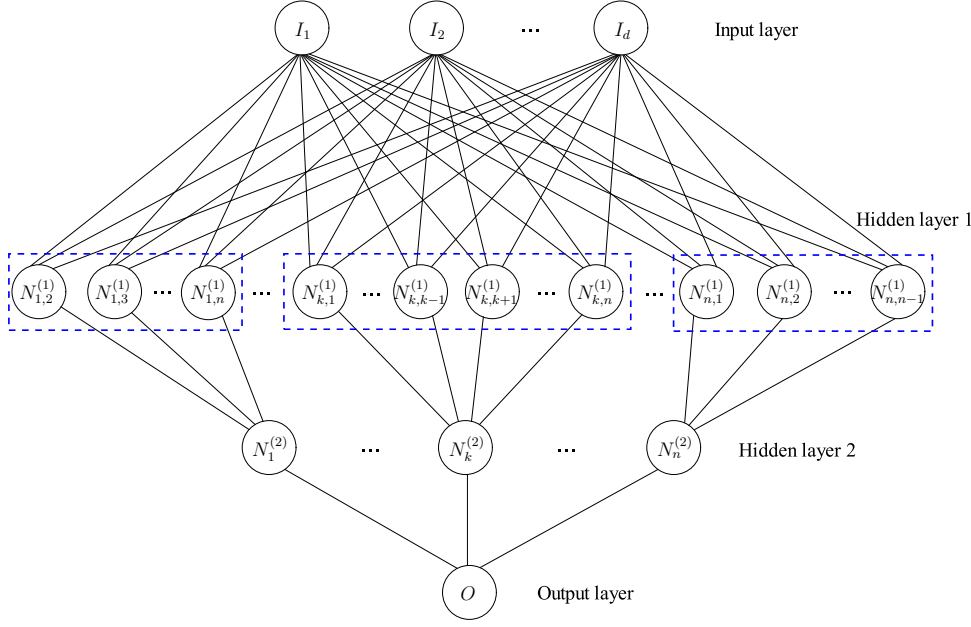


FIG. 3.1. The schematic diagram of the FNN with two hidden layers.

where the first index $k = 1, \dots, n$, denotes the k -th group, and the second index $j \neq k$ denotes its location within the k -th group. Note that this is merely an indexing scheme to distinctly identify the neurons. The neurons have no lateral connections and each receive the same signals from the input layer, as illustrated in Fig. 3.1.

The output of the neurons in the first hidden layer is explicitly defined as follows,

$$z_{k,j}^{(1)}(\mathbf{x}) = s(\mathbf{w}_{k,j} \cdot \mathbf{x} - b_{k,j}), \quad 1 \leq k \leq n, \quad 1 \leq j \leq n, \quad j \neq k, \quad (3.2)$$

where

$$\begin{aligned} \mathbf{w}_{k,j} &= \mathbf{x}^{(k)} - \mathbf{x}^{(j)}, \\ b_{k,j} &= \frac{1}{2}(\mathbf{x}^{(k)} - \mathbf{x}^{(j)}) \cdot (\mathbf{x}^{(k)} + \mathbf{x}^{(j)}). \end{aligned} \quad (3.3)$$

Here $\mathbf{x}^{(k)}$ are the coordinates of the k -th training sample (2.1). Obviously, $z_{k,j}^{(1)} \in \{0, 1\}$ because of the use of the binary activation function. We write

$$\mathbf{z}_k^{(1)}(\mathbf{x}) = \left(\dots, z_{k,k-1}^{(1)}, z_{k,k+1}^{(1)}, \dots \right)^\top \in \{0, 1\}^{n-1}, \quad 1 \leq k \leq n, \quad (3.4)$$

as the output vector of the k -th group, $1 \leq k \leq n$.

3.1.2. Second hidden layer. The second hidden layer consists of n neurons, each of which only receives the output signals from a unique group in the first hidden layer, as illustrated in Figure 3.1. The output of each neuron in the second hidden layer is defined as,

$$z_k^{(2)}(\mathbf{x}) = s(\mathbf{1} \cdot \mathbf{z}_k^{(1)}(\mathbf{x}) - b^{(2)}), \quad k = 1, \dots, n, \quad (3.5)$$

where

$$\mathbf{1} = (1, \dots, 1)^\top \in \mathbb{R}^{n-1}, \quad b^{(2)} = n - 1, \quad (3.6)$$

and $\mathbf{z}_k^{(1)}(\mathbf{x})$ is the output vector from the k -th group in the first layer, as defined in (3.4). To avoid the unexpected effect of computer round-off error, during implementation one may define $b^{(2)} = n - 1 - \epsilon$, where $0 < \epsilon < 1$ is an arbitrary constant. It is obvious $z_k^{(2)}(\mathbf{x}) \in \{0, 1\}$, $k = 1, \dots, n$.

3.1.3. Output layer. The output layer receives signals from all the neurons in the second hidden layer, as shown in Figure 3.1. It produces the final output as follow,

$$y(\mathbf{x}) = \sum_{k=1}^n f^{(k)} \cdot z_k^{(2)}(\mathbf{x}), \quad (3.7)$$

where $f^{(k)}$, $k = 1, \dots, n$, are the sample data.

3.2. Approximation property. It is straightforward to show that the outputs of the two hidden layers (3.5) effectively produce a Voronoi diagram for the underlying domain D , where the function f is defined, and the final output (3.7) thus becomes a piecewise constant approximation of f based on the Voronoi diagram. To proceed, we first invoke the concept of (ordinary) Voronoi diagram (cf. [10]).

DEFINITION 3.1 (Voronoi diagram). For points $X = \{\mathbf{x}^{(1)}, \dots, \mathbf{x}^{(n)}\} \subset D \subseteq \mathbb{R}^d$, where $2 \leq n < \infty$ and $\mathbf{x}^{(i)} \neq \mathbf{x}^{(j)}$ for $i \neq j$. We call the region

$$V^{(i)} = \left\{ \mathbf{x} \mid \|\mathbf{x} - \mathbf{x}^{(i)}\|_2 \leq \|\mathbf{x} - \mathbf{x}^{(j)}\|_2, \quad \forall j \neq i \right\} \quad (3.8)$$

the ordinary Voronoi cell associated with $\mathbf{x}^{(i)}$, and the set $\mathcal{V}(X) = \{V^{(1)}, \dots, V^{(n)}\}$ the ordinary Voronoi diagram generated by X .

THEOREM 3.2. The output of the FNN (3.7) is a piecewise constant approximation to the function $f(x)$ using the training data set $\{\mathbf{x}^{(k)}, f(\mathbf{x}^{(k)})\}_{k=1}^n$. More precisely, for $n \geq 2$,

$$y(\mathbf{x}) = \sum_{k=1}^n f(\mathbf{x}^{(k)}) \mathbb{I}_{V^{(k)}}(\mathbf{x}), \quad (3.9)$$

where $V^{(k)}$ is the Voronoi cell associated by the point $\mathbf{x}^{(k)}$, and $\mathbb{I}_A(\mathbf{x})$ is the indicator function for a set A satisfying

$$\mathbb{I}_A(\mathbf{x}) = \begin{cases} 1, & \mathbf{x} \in A, \\ 0, & \mathbf{x} \notin A. \end{cases}$$

Proof. For each $\mathbf{x}^{(k)}$, $k = 1, \dots, n$, $n \geq 2$, consider $\mathbf{x}^{(j)}$, $j \neq k$. Let

$$\mathbf{x}_{k,j}^{mid} = \frac{1}{2}(\mathbf{x}^{(k)} + \mathbf{x}^{(j)})$$

be the mid-point between the two points $\mathbf{x}^{(k)}$ and $\mathbf{x}^{(j)}$. Then, the output of the first hidden layer (3.2) $z_{k,j}^{(1)} = 1$, if and only if,

$$(\mathbf{x}^{(k)} - \mathbf{x}^{(j)}) \cdot \mathbf{x} \geq (\mathbf{x}^{(k)} - \mathbf{x}^{(j)}) \cdot \mathbf{x}_{j,k}^{mid},$$

which is equivalent to

$$(\mathbf{x} - \mathbf{x}_{j,k}^{mid}) \cdot (\mathbf{x}^{(k)} - \mathbf{x}^{(j)}) \geq 0. \quad (3.10)$$

Note that

$$\{\mathbf{x} \mid (\mathbf{x} - \mathbf{x}_{j,k}^{mid}) \cdot (\mathbf{x}^{(k)} - \mathbf{x}^{(j)}) = 0\}$$

is the center hyperplane separating the two points $\mathbf{x}^{(k)}$ and $\mathbf{x}^{(j)}$. Therefore, (3.10) contains all the points that are closer to $\mathbf{x}^{(k)}$ than to $\mathbf{x}^{(j)}$. We then have, for each $1 \leq k \leq n$ and $j \neq k$,

$$\{\mathbf{x} \mid z_{k,j}^{(1)}(\mathbf{x}) = 1\} = \{\mathbf{x} \mid \|\mathbf{x} - \mathbf{x}^{(k)}\|_2 \leq \|\mathbf{x} - \mathbf{x}^{(j)}\|_2\}.$$

The output of the k th neuron in the second hidden layer (3.5) satisfies

$$z_k^{(2)} = 1, \quad \text{if and only if,} \quad \mathbf{z}_k^{(1)} = \mathbf{1},$$

where again $\mathbf{1} = (1, \dots, 1)^T \in \mathbb{R}^{n-1}$ is a vector of length $(n-1)$. This is equivalent to $z_{k,j}^{(1)} = 1, \forall j \neq k$. Therefore,

$$\{\mathbf{x} \mid z_{k,j}^{(2)}(\mathbf{x}) = 1\} = \{\mathbf{x} \mid \|\mathbf{x} - \mathbf{x}^{(k)}\|_2 \leq \|\mathbf{x} - \mathbf{x}^{(j)}\|_2, \forall j \neq k\} = V^{(k)},$$

which is, by definition, the Voronoi cell associated with the point $\mathbf{x}^{(k)}$. The output of the network (3.7) is obviously a piecewise constant function in the form of (3.9). \square

If one assumes certain differentiability condition on the target function f , then we have the following result on the error estimate in L^2 norm. More specifically, we define the L^2 norm with respect to a measure $\mu(\mathbf{x})$,

$$\|f\|_{L^2_{d\mu}(D)} := \left(\int_D f^2(\mathbf{x}) d\mu(\mathbf{x}) \right)^{1/2}. \quad (3.11)$$

We assume that the volume of D with respect to μ is a finite constant, and without loss of generality, we set this constant to be 1. That is,

$$\int_D d\mu(\mathbf{x}) = 1.$$

THEOREM 3.3. *Assume $f(\mathbf{x})$ is differentiable and with bounded first-order derivatives, and the measure μ is such that*

$$\int_D \|\mathbf{x}\|_2^2 d\mu(\mathbf{x}) < \infty.$$

Then, the approximation error of the FNN (3.7) satisfies

$$\|y - f\|_{L^2_{d\mu}(D)} \leq \left(\sup_{\mathbf{x} \in D} \|\nabla f(\mathbf{x})\|_2 \right) \left(\sum_{i=1}^n \int_{V^{(i)}} \|\mathbf{x}^{(i)} - \mathbf{x}\|_2^2 d\mu(\mathbf{x}) \right)^{\frac{1}{2}}. \quad (3.12)$$

Proof. From (3.9), we have

$$\begin{aligned}
\|y - f\|_{L^2_{d\mu}(D)}^2 &= \sum_{i=1}^n \int_{V^{(i)}} |f(\mathbf{x}^{(i)}) - f(\mathbf{x})|^2 d\mu(\mathbf{x}) \\
&= \sum_{i=1}^n \int_{V^{(i)}} \left| \int_0^1 (\mathbf{x}^{(i)} - \mathbf{x}) \cdot \nabla f(t\mathbf{x}^{(i)} + (1-t)\mathbf{x}) dt \right|^2 d\mu(\mathbf{x}) \\
&\leq \sum_{i=1}^n \int_{V^{(i)}} \left(\|\mathbf{x}^{(i)} - \mathbf{x}\|_2 \int_0^1 \|\nabla f(t\mathbf{x}^{(i)} + (1-t)\mathbf{x})\|_2 dt \right)^2 d\mu(\mathbf{x}) \\
&\leq \sum_{i=1}^n \left(\sup_{\mathbf{x} \in V^{(i)}} \|\nabla f(\mathbf{x})\|_2 \right)^2 \int_{V^{(i)}} \|\mathbf{x}^{(i)} - \mathbf{x}\|_2^2 d\mu(\mathbf{x}) \\
&= \left(\sup_{\mathbf{x} \in D} \|\nabla f(\mathbf{x})\|_2 \right)^2 \sum_{i=1}^n \int_{V^{(i)}} \|\mathbf{x}^{(i)} - \mathbf{x}\|_2^2 d\mu(\mathbf{x}).
\end{aligned}$$

The proof is then completed. \square

COROLLARY 3.4. *Under the hypotheses of Theorem 3.3, if D is bounded and μ is uniform measure, then*

$$\|y - f\|_{L^2_{d\mu}(D)} \leq \left(\sup_{\mathbf{x} \in D} \|\nabla f(\mathbf{x})\|_2 \right) \delta, \quad (3.13)$$

where

$$\delta := \max_{1 \leq i \leq n} \text{diam}(V^{(i)}),$$

with $\text{diam}(A) := \sup_{\mathbf{x}, \mathbf{x}' \in A} \|\mathbf{x} - \mathbf{x}'\|_2$ denoting the diameter of a bounded set A .

Proof. The conclusion directly follows from Theorem 3.3, because

$$\sum_{i=1}^n \int_{V^{(i)}} \|\mathbf{x}^{(i)} - \mathbf{x}\|_2^2 d\mu(\mathbf{x}) \leq \delta^2 \sum_{i=1}^n \int_{V^{(i)}} d\mu(\mathbf{x}) = \delta^2.$$

\square

Note that, if the training data points $\{\mathbf{x}^{(j)}\}_{j=1}^n$ are (almost) uniformly distributed in the bounded domain D , then $\delta \sim n^{-\frac{1}{d}}$, c.f., [8]. This implies that the error of our FNN scales as

$$\|y - f\|_{L^2_{d\mu}(D)} \sim \mathcal{O}(n^{-\frac{1}{d}}). \quad (3.14)$$

4. Numerical Examples. In this section we present numerical examples to demonstrate the properties of our FNN. Upon explicitly constructing the FNN using training data, all numerical errors are computed using another set of samples — a validation sample set. In all our examples, the validation set consists of M randomly generated points that are independent of the training set. The size M is taken as 200 and 10,000, for univariate and multivariate tests, respectively. We compute the differences between the FNN approximations and the true functions on the validation sets and report both their ℓ_∞ vector norm and ℓ_2 vector norm, denoted as ϵ_∞ error and ϵ_2 error, respectively.

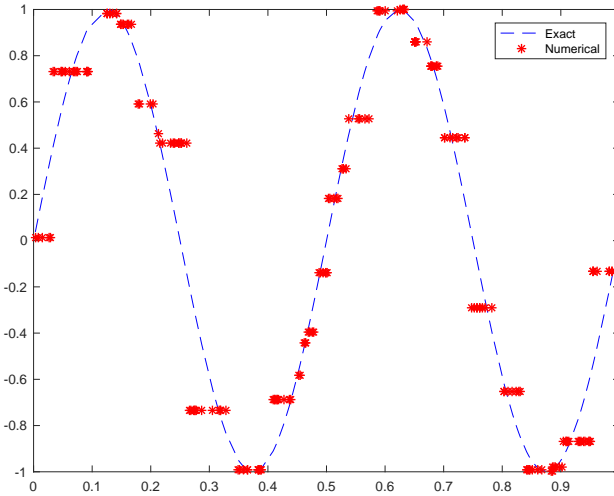


FIG. 4.1. Approximation of $f(x) = \cos(4\pi x)$ using $n = 32$ random training data.

4.1. Univariate functions. We first consider a simple smooth function $f(x) = \sin(4\pi x)$, $x \in [0, 1]$. Fig. 4.1 shows the FNN approximation of this function with $n = 32$ randomly generated training samples. The numerical approximation by the FNN is clearly a piecewise constant approximation of the exact function.

We then examine the errors in the FNN approximation with respect to increasing number of the training data n . The errors are shown in Fig. 4.2, using both uniformly distributed training data (left figure) and randomly generated training data (right figure). The n^{-1} error convergence rate is clearly visible, consistent with the estimate in Theorem 3.3.

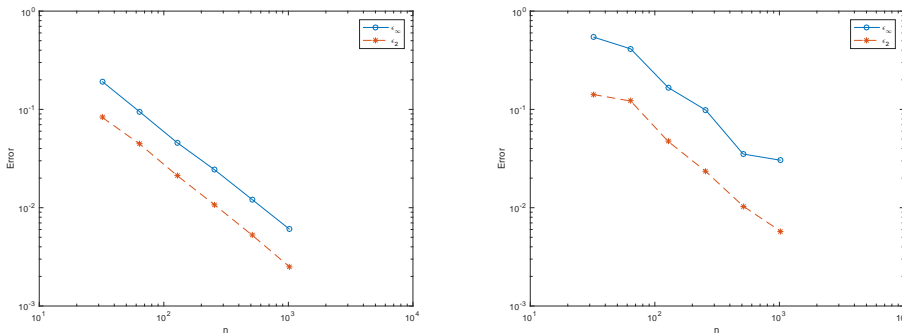


FIG. 4.2. Errors vs. n for 1d cosine function. Left: uniform training data; Right: random training data.

Next we consider a univariate discontinuous function, which is rather arbitrarily chosen as

$$f(x) = 3s(x - 0.313) + s(x - 0.747) + 2 \cos(4\pi x), \quad x \in [0, 1],$$

where $s(x)$ is the step function (3.1). The left of Fig. 4.3 shows the FNN approximation using $n = 1,024$ uniformly distributed training samples, whereas the right of Fig. 4.3 shows the error decay with respect to the number of training samples. We observe good approximation property and expected convergence rate from (3.14).

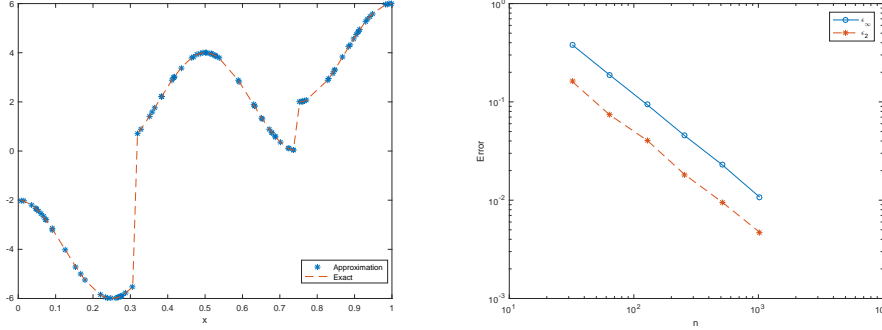


FIG. 4.3. Approximation of a discontinuous function in 1d with uniform training data. Left: Function approximation with $n = 1,024$ training samples; Right: Errors vs. number of training samples n .

4.2. Multivariate functions. We now consider multivariate functions. Throughout this section, all training samples are generated randomly using uniform distribution. Two functions are examined, a sine function and a Gaussian function, in the following form,

$$f_S(\mathbf{x}) = \sin\left(\omega \sum_{i=1}^d x_i\right), \quad \mathbf{x} \in [0, 1]^d, \quad f_G(\mathbf{x}) = \exp\left(-\sum_{i=1}^d \left(\frac{x_i}{2}\right)^2\right), \quad \mathbf{x} \in [-1, 1]^d.$$

First, we consider the functions in 2-dimension ($d = 2$). The numerical errors induced by our FNN for these two functions are plotted in Fig. 4.4, with respect to the number of training samples. We observe the expected rate of error convergence (3.14).

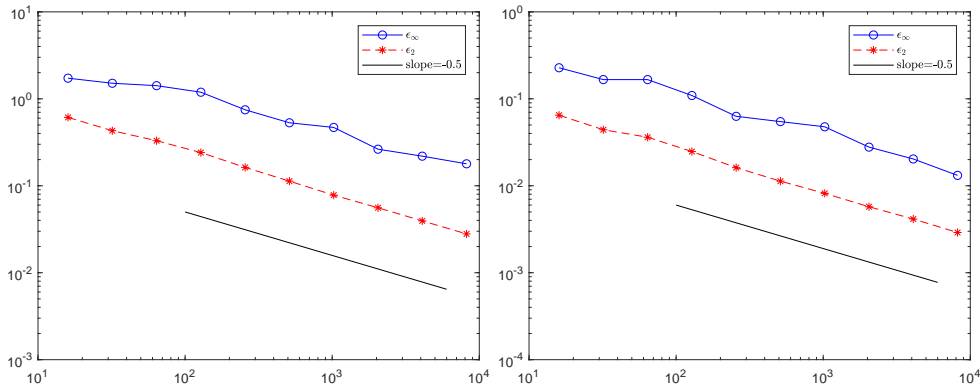


FIG. 4.4. Approximation errors of the sine and Gaussian functions in $d = 2$ versus number of training samples. Left: f_S with $\omega = 2\pi$; Right: f_G .

Next, we consider functions in $d = 4$ dimensions. The numerical errors induced by our FNN are plotted in Fig. 4.5, with respect to the number of training samples. Again, we observe expected error behavior (3.14).

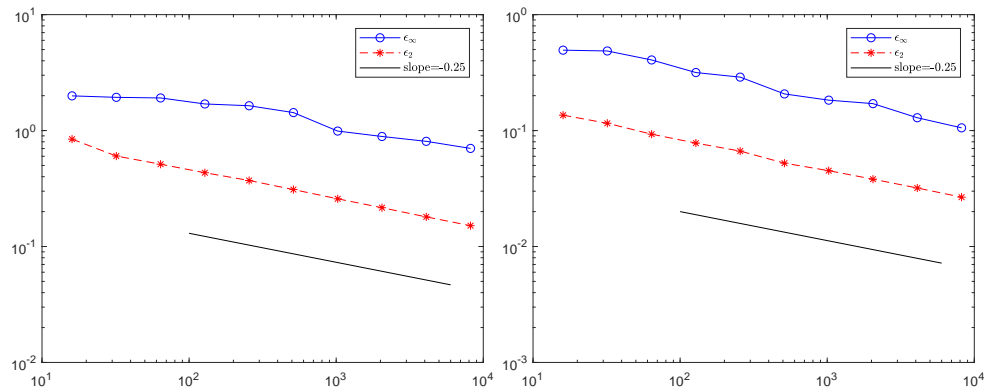


FIG. 4.5. Approximation errors of the sine and Gaussian functions in $d = 4$ versus number of training samples. Left: f_S with $\omega = \pi$; Right: f_G .

5. Summary. In this paper we presented a new explicit construction of feedforward neural network (FNN). Our network consists of two hidden layers and uses the step function as the activation function. It is able to construct a Voronoi diagram of a given multivariate domain and provides a piecewise constant approximation of any function defined in the domain. Our construction uses n^2 neurons, where n is the number of training samples. It is worth noting that it is possible to construct a similar piecewise constant approximation FNN using a smaller number (less than n^2) of neurons. That, however, would require more complex signal pathways among the neurons, with potential lateral connections within the layers. Our current construction represents perhaps the most straightforward construction of this type. In addition to being another (new) constructive proof, from the mathematical view point, for the universal approximation properties of FNNs, our construction is also practical and can be easily adopted for applications.

REFERENCES

- [1] G.A. Anastassiou. Rate of convergence of some neural network operators to the unit-univariate case. *J. Math. Anal. Appl.*, 212:237–262, 1997.
- [2] A.R. Barron. Universal approximation bounds for superpositions of a sigmoidal function. *IEEE Trans. Info. Theory*, 39(3):930–945, 1993.
- [3] F. Cao, Y. Zhang, and Z.-R. He. Interpolation and rates of convergence for a class of neural networks. *App. Math. Model.*, 33:1441–1456, 2009.
- [4] P. Cardaliaguet and G. Euvrard. Approximation of a function and its derivative with a neural network. *Neural Networks*, 5:207–220, 1992.
- [5] D. Costarelli. Neural network operators: constructive interpolation of multivariate functions. *Neural Networks*, 67:28–36, 2015.
- [6] D. Costarelli and R. Spigler. Constructive approximation by superposition of sigmoidal functions. *Analysis Theory Appl.*, 29(2):169–196, 2013.
- [7] G. Cybenko. Approximation by superpositions of a sigmoidal function. *Math. Control Signal Sys.*, 2:207–220, 1989.
- [8] Luc Devroye, László Györfi, Gábor Lugosi, and Harro Walk. On the measure of Voronoi cells. *J. Appl. Prob.*, 54(2):394–408, 2017.

- [9] B. Llanas and F.J. Sainz. Constructive approximate interpolation by neural networks. *J. Comput. Applied Math.*, 188:283–308, 2006.
- [10] A. Okabe, B. Boots, and K. Sugihara. *Spatial tessellations: concepts and applications of Voronoi diggrams*. John Wiley & Sons Ltd., 1992.
- [11] A. Pinkus. Approximation theory of the MLP model in neural networks. *Act. Numer.*, pages 143–195, 1999.